



Biophysical Studies on the Interactions of Nitrofurantoin with Bovine Serum Albumin by Spectroscopic and Molecular Modeling Methods

S. Harsha, K. R. Punyashree, T. N. Vidyashree, B. M. Krupa,
Babu Giriya Gowda* R. NageshBabu and F. Shafia Hoor

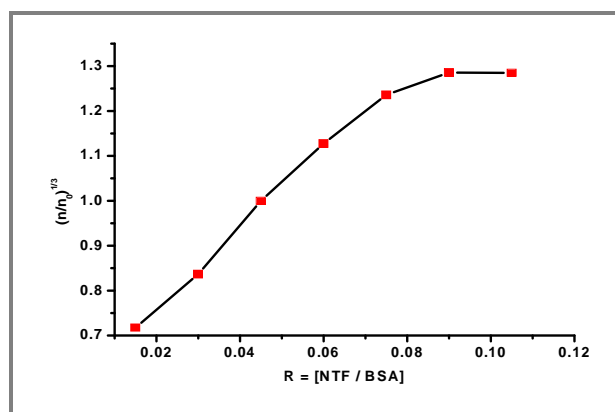
Department of Chemistry, Maharani's Science College for Women, Bangalore-01, **INDIA**
Email: babgowda@gmail.com

Accepted on 9th August, 2020

ABSTRACT

The interaction between nitrofurantoin (NTF) and bovine serum albumin (BSA) has been studied. The studies were carried out in a buffer medium of pH 7.4 using fluorescence spectroscopy, UV-Vis spectroscopy, Viscometry and molecular modeling methods. The results of fluorescence quenching and UV-Vis absorption spectra experiments indicated the formation of the complex of BSA-NTF. Binding parameters were determined using the Stern-Volmer equation. From fluorescence and UV-Vis spectroscopic data, the binding constant between NTF and BSA was calculated to be $4.275 \times 10^3 \text{ L mol}^{-1}$ and $8.173 \times 10^3 \text{ L mol}^{-1}$ respectively. The results of thermodynamic parameters ΔG° , ΔH° and ΔS° at different temperature indicate that the electrostatic interactions and also hydrogen bonds play a major role for NTF-BSA association. Molecular modeling calculation demonstrated that NTF is mainly located within the hydrophobic pocket of the subdomain IIIA of BSA.

Graphical Abstract



Effect of increasing the concentration of BSA on the relative viscosity of NTF.

Keywords: Nitrofurantoin macrocrystals, BSA, Spectroscopic, Molecular modelling.

INTRODUCTION

The drug–protein binding constant is a physicochemical parameter that helps us to understand the absorption, transport, and the target molecules of the drugs at the cellular level [1, 2]. Serum albumin is one of the main extracellular proteins, with a high concentration in blood plasma, present in 6.0×10^{-4} M, contributes to about 80 % of the blood osmotic pressure [3, 4]. Bovine serum albumin (BSA) is homologous, having ~88 % sequence homology, with human serum albumin and is the major soluble protein component of the blood serum of cow. The remarkable binding properties of serum albumin account for the central role in both the efficacy and rate of delivery of drugs [5–7]. Therefore, the studies on the binding of drugs to serum albumin become an important research field in chemistry, life science and clinical medicine [8–10]. Plenty of studies on the interactions between serum albumin with internal compounds and pharmaceutical molecules have been carried out [11–13], and are considered to further broaden the perspective on the scientific research of drug in interdisciplinary fields.

Nitrofurantoin (Figure 1) [1-(5-nitro-2-furfurylidene aminohydantoin)] is a synthetic, nitrofuran derivative antibacterial agent. This drug is usually bacteriostatic but may be bactericidal in action, depending on its concentration attained at the site of infection and the susceptibility of the infecting organism [14]. It is used in the treatment of initial or recurrent urinary tract infections caused by susceptible organisms. This drug is active against many gram-negative and some gram-positive bacteria including *Citrobacter*, *Corynebacterium*, *Enterobacter*, *Escherichia coli*, *Klebsiella*, *Neisseria*, *Salmonella*, *Shigella*, *Staphylococcus aureus* and *Enterococcus faecalis*. In general, most susceptible bacteria are inhibited in vitro by Nitrofurantoin concentrations of $1\text{--}32 \text{ g mL}^{-1}$. Higher concentrations of the drug may be required to inhibit some strains of *Enterobacter* and *Klebsiella* [14].

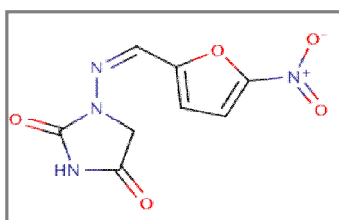


Figure 1. Structure of Nitrofurantoin.

In spite of these broad pharmacological uses of NTF mentioned above, its effects on plasma protein and the mechanism of action has seldom been reported. In the present work, spectroscopic, viscometric and molecular modeling approaches were performed in order to elucidate the site selective binding of NTF to BSA. The interaction information regarding quenching mechanisms, binding parameters, thermodynamic parameters, binding modes, site-selective binding site, and conformation investigation is reported here.

MATERIALS AND METHODS

Materials and Methods: Bovine serum albumin (BSA) was purchased from Sigma Chemical Company, St.Louis, USA and used without purification. Nitrofurantoin (NTF) was obtained from sigma Aldrich, India. The solutions of NTF and BSA were prepared in 0.1M phosphate buffer of pH7.4 with respect to their molecular weight and stored at 4°C . All other chemicals were of analytical reagent grade and Millipore water was used throughout the work.

Instrumentation: All of the fluorescence measurements were carried out on a F-2700 recording spectrofluorometer (Hitachi, Japan) equipped with a 150 W Xenon lamp source and 1.0 cm quartz cells. The excitation and emission bandwidths were both 5 nm. An Ellico UV-Visible

spectrophotometer equipped with a 1.0 cm cuvette was used to scan the UV spectrum. All of the pH measurements were made with Scott Gerate pH meter CG 804. The viscosity measurements were made with viscometer which was immersed in a thermostat water-bath at room temperature.

UV-Vis Spectra measurements: The UV measurements of NTF in the presence and absence of BSA were made in the range of 210-300 nm. NTF concentration was fixed at $1.5 \times 10^{-4} \text{ M L}^{-1}$ while the BSA concentration was varied from 0 to $30 \times 10^{-6} \text{ M L}^{-1}$ in presence of phosphate buffer of pH 7.4 at 298 K.

Fluorescence Spectra measurements: A solution of NTF ($1.5 \times 10^{-4} \text{ M}$) was titrated by successive additions of a stock solution of BSA ($8.0 \times 10^{-5} \text{ M L}^{-1}$). Each solution was allowed to reach equilibrium for 5 min. The fluorescence spectra of the mixtures were then recorded in the wavelength range of 310–530 nm when excited with $\lambda_{\text{ex}} = 365 \text{ nm}$. The emission spectra were recorded at three different temperatures, i.e., 293, 303 and 310 K.

Viscosity measurements: Viscometric titrations were made using a viscometer, which was immersed in a thermostatic water-bath at 25°C. The experiments were conducted by adding appropriate amounts of NTF into the viscometer to give a certain $r(=[\text{NTF}]/[\text{BSA}])$ value while keeping the BSA concentration constant. The flow time of the solution through the capillary was measured with an accuracy of $\pm 0.20 \text{ s}$ by using a digital stop watch. The mean values of three replicate measurements were used to evaluate the average relative viscosity of the sample. The data were presented as $(\eta/\eta_0)^{1/3}$ versus $r^{1/2}$, where η and η_0 are the viscosities of BSA in the presence and absence of NTF, respectively. Viscosity values were calculated from the observed flow time of BSA-containing solutions (t) and corrected for buffer solution (t_0), $\eta = (t - t_0)/t_0$.

Molecular modeling: The Molecular docking studies of BSA with compounds were achieved by using Auto dock Vina, developed at the Scripps research institute (<http://vina.scripps.edu>) [15]. The input files for AutoDock Vina were prepared with AutoDock Tools (ADT), which is a Graphical User Interface for AutoDock and AutoDock Vina. The crystal structure of Bovine Serum Albumin (3V03) was retrieved from Protein Data Bank and the Ligand Binding Site location was analysed by Q-Site Finder [16]. The co-crystallized ligand was removed. Using ADT the water molecules were removed from the protein and polar hydrogen were added followed by adding Kollman charges. The Grid box has been set according to the binding site on protein and saved as pdbqt format, which was required by AutoDock Vina. The 2 dimensional structure of ligand were drawn by Chem sketch and converted to PDB format, required by AutoDock Tools by Open Babel [17]. The rotatable bonds were selected within the ligand using Choose Torsions option in ADT and saved in pdbqt format. The Lamarckian Genetic Algorithm (LGA), which is a novel and robust automated docking method available in AutoDock [18], was employed.

RESULTS AND DISCUSSION

UV-Vis Absorption Spectroscopy: Figure 2(a) showed the UV/Vis absorption spectra of NTF in the absence and presence of different concentrations of BSA. The maximum absorbance of NTF was located around at 365 nm. It was observed that on the addition of BSA, NTF showed a decrease in molar absorptivity with a red shift of 1-5 nm. This hypochromic effect is thought to be due to the interaction between the electronic states of the intercalating chromophore and those of the BSA bases [19]. Generally, the blue shift (or red shift), hyperchromic (or hypochromic) effects are the properties of BSA-drug interaction which are closely related with double helix structure [20]. The NTF solution exhibited peculiar hypochromic effect and bathochromic shift in UV/Vis spectra upon binding to BSA, a typical characteristic of an intercalating mode [19].

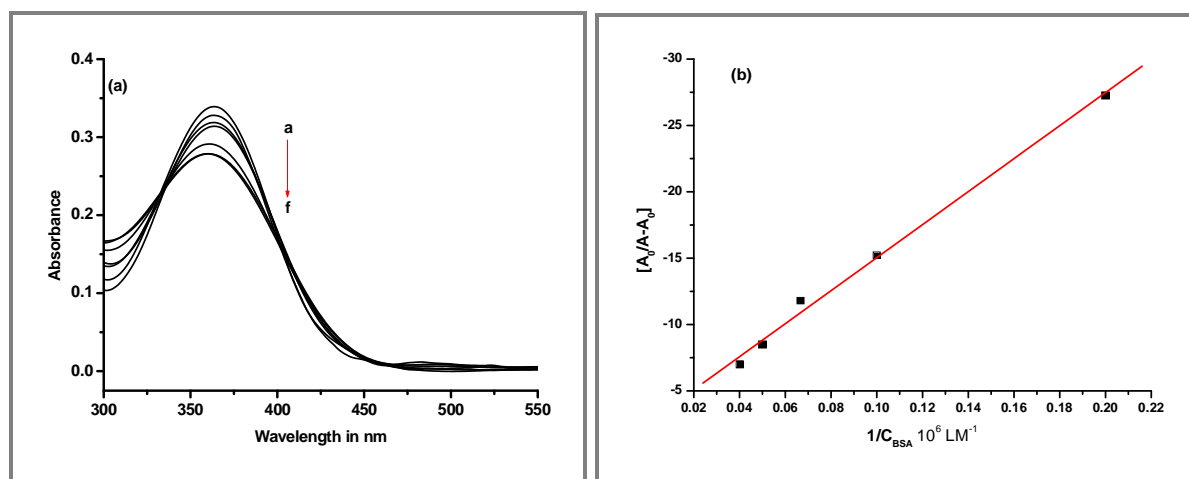


Figure 2. (a) UV-visible spectra of 1.5×10^{-4} M NTF in the presence of $C_{\text{BSA}} = 0, 5, 10, 15, 20, 25$ and $30 \mu\text{M L}^{-1}$ BSA (a to f) in buffer of pH-7.4 and (b) Plot of $(A_0 / (A - A_0))$ versus $1 / [\text{BSA}]$ for NTF - BSA system.

Based on the variations in absorbance spectra of NTF upon binding to BSA, the binding constant (K) was calculated according to the following equation [21].

$$\frac{A_0}{A - A_0} = \frac{\epsilon_G}{\epsilon_{\text{H-G}} - \epsilon_G} + \frac{\epsilon_G}{\epsilon_{\text{H-G}} - \epsilon_G} \times \frac{1}{K [\text{BSA}]}$$

Where, A_0 and A are the absorbance of drug in the absence and presence of BSA, ϵ_G and $\epsilon_{\text{H-G}}$ are the absorption coefficients of drug and its complex with BSA, respectively. The plot of $A_0/(A - A_0)$ versus $1/[\text{BSA}]$ was constructed (Figure 2b) using the data from the absorbance titrations and a linear fitting of the data yielded the binding constants (K) ($8.173 \times 10^3 \text{ LM}^{-1}$) for NTF-BSA. These results are close to that from spectrofluorimetry.

Fluorescence quenching spectra: The binding of NTF to BSA was also examined by fluorescence titration measurement. NTF shows strong fluorescence emission peak at 479 nm ($\lambda_{\text{ex}} = 365 \text{ nm}$). An obvious decrease of the fluorescence intensity of NTF was observed with increasing of BSA concentration (Figure 3). This shows that NTF fluorescence is efficiently quenched upon binding to BSA.

Quenching mechanism and Binding Constants: A quenching process can be usually induced by a collisional process which is dynamic quenching or a formation of a complex between quencher and fluorophore which is static quenching. Dynamic quenching depends upon diffusion. Since higher temperatures results in larger diffusion coefficients, the biomolecular quenching constants are expected to increase with increasing temperature. In contrast, an increase in temperature is likely to result in a decrease in stability of complexes, and thus lower values of the static quenching constants [22]. In order to confirm the quenching mechanism, the fluorescence quenching was analysed according to the Stern-Volmer equation [23].

$$F_0 / F = 1 + k_q \tau_0 [Q] = 1 + K_{\text{sv}} [Q] \quad \dots(1)$$

Where, F_0 and F represent the steady-state fluorescence intensities in the absence and presence of quencher, respectively. $[Q]$ is the concentration of quencher. k_q is the quenching rate constant of biomolecule. τ_0 is life time of biomolecule without the quencher and its value is 10^{-8} s [24], and K_{sv} is the Stern-Volmer dynamic quenching constant, which was determined by linear regression of a plot of F_0/F against $[Q]$. According to Eq. 2, the quenching constant k_q was calculated to be about $10^{11} \text{ L mol}^{-1}$ as listed in table 1. However, the maximum scatter collision quenching constant k_q of various

quencher with the biopolymer is $2.0 \times 10^{10} \text{ L mol}^{-1} \text{ s}^{-1}$ [25], which suggests that the fluorescence quenching process may be mainly controlled by a static quenching mechanism rather than dynamic. From table 1 we can also clearly see that K_{SV} is inversely correlated with temperature which indicates again that the quenching is not caused by dynamic collision but comes from the formation of a complex. So fluorescence quenching mechanism of NTF by BSA is a static quenching type.

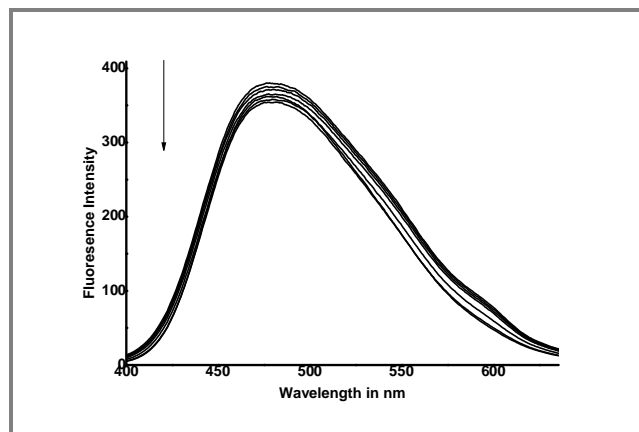


Figure 3. Fluorescence spectra of $1.5 \times 10^{-4} \text{ M}$ NTF in the presence of $C_{\text{BSA}} = 0, 5, 10, 15, 20, 25.0, 30, 35 \mu\text{M L}^{-1}$ BSA in phosphate buffer solution of pH-7.4.

The binding constant K and the number of binding sites n of NTF with BSA are calculated by the following equation using the data from fluorescence titration:

$$\text{Log} (F_0 - F) / F = \text{log}K_b + n \text{log} [Q] \quad \dots(2)$$

Where in the present case, K_b is the binding constant and n is the number of binding sites, which can be determined by the ordinate and slope of double logarithm regression curve (Figure 4) of $\text{log} (F_0 - F)$ versus $\text{log} [Q]$ based on the eq.2, respectively. The values of K_b and n are evaluated and presented in table 1. From table 1, it can be found that NTF may effectively bind to BSA with high affinity, and the ratio of binding of BSA to NTF is about 1:3. Additionally, we can also see that the values of K_b decrease with the increase in temperature, which is in good agreement with the trend of K_{SV} as mentioned above. It implies that an unstable complex may be formed in the binding reaction and the complex would possibly be dissociated partly when the temperature increases.

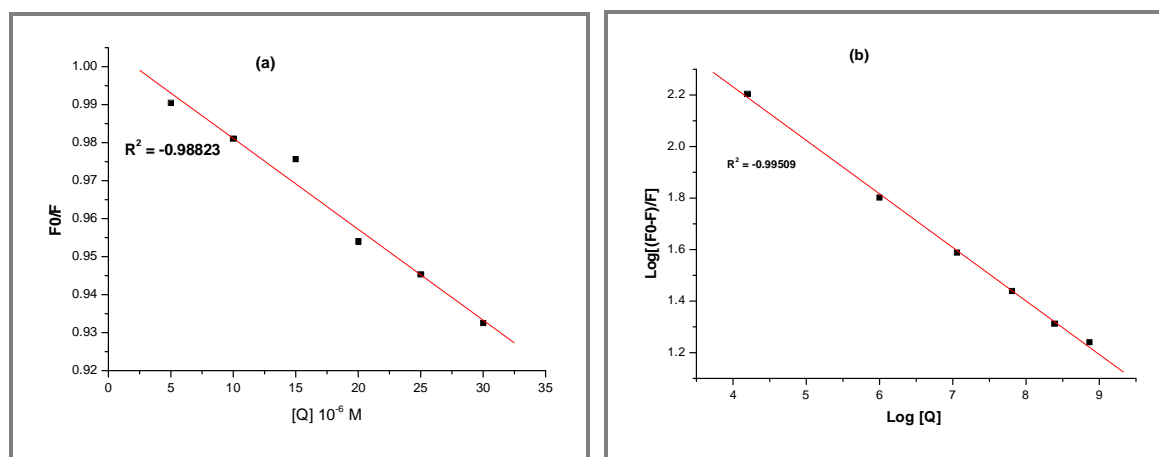


Figure 4. (a) Stern-Volmer plot of (F / F_0) vs. $[Q]$ for NTF-BSA system and (b) Plot of $\text{log} [(F_0 - F)/F]$ vs. $\text{log} [Q]$ for NTF-BSA system.

Table 1. The dynamic quenching constants between NTF and BSA at different temperatures

T (K)	K_{SV} (L mol ⁻¹)	k_q (L mol ⁻¹ s ⁻¹)	K_b (L mol ⁻¹)	n	R ^a
293	3.338 x 10 ³	3.3375 x 10 ¹¹	4.275 x 10 ³	1.579	0.9882
303	2.956 x 10 ³	3.341 x 10 ¹¹	6.714 x 10 ³	1.497	0.9803
310	2.617 x 10 ³	2.623 x 10 ¹¹	5.128 x 10 ³	1.441	0.9871

R^a is the correlation coefficient

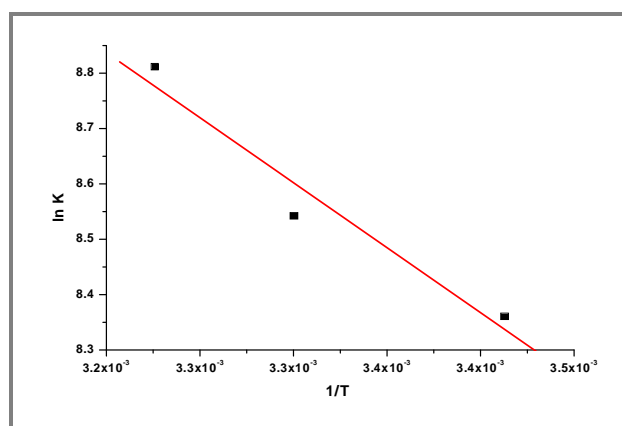
Binding Mode: The acting forces between a small molecular substance and BSA mainly include hydrogen bond, van der Waals force, electrostatic force, hydrophobic interaction force and so on. The signs and magnitudes of thermodynamic parameters for BSA interactions can account for the main forces contributing to BSA stability [26, 27]. If the enthalpy changes (ΔH^0) do not vary significantly over the temperature range studied, then its value could be determined from Van't Hoff equation [28]:

$$\ln K = -\Delta H^0 / RT + \Delta S^0 / R \quad \dots(3)$$

The free energy change ΔG^0 of the binding reaction at different temperature was estimated from the eq. 4:

$$\Delta G^0 = \Delta H^0 - T \Delta S^0 \quad \dots(4)$$

From the linear relationship between $\ln K$ and $1/T$, the value of ΔH^0 and ΔS^0 could be obtained (Figure 5). The ΔG^0 at different temperatures were calculated using eq. 4, the results were presented in table 2.

**Figure 5.** Van't Hoff plots of $\ln K$ vs. $1/T$.

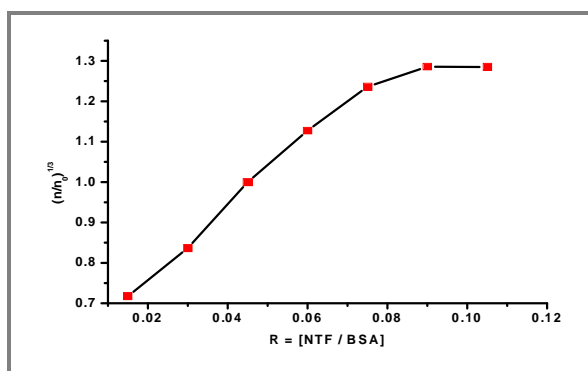
Many references have reported the characteristic sign of the thermodynamic parameter associated with the various individual kinds of interaction that may take place in macromolecules association process [29]. The thermodynamic parameters (ΔH , ΔS) before and after reaction can be used to determine the type of interaction: when $\Delta H > 0$, $\Delta S > 0$, the acting force was hydrophobic force; when $\Delta H < 0$, $\Delta S < 0$ it was van der Waals' force and hydrogen bond; and when $\Delta H < 0$, $\Delta S > 0$, it was electrostatic force [30, 31]. It was displayed in Table 2 that the fact $\Delta G < 0$ proved that the reaction was spontaneous, and that $\Delta H > 0$, $\Delta S > 0$ proved the acting force type was hydrophobic force.

Viscosity Measurements: Viscosity experiment is an effective tool to study the binding mode of small molecules to BSA. The interaction between NTF and BSA, we carried out viscosity measurements at room temperature. A classical intercalation binding demands the space adjacent base pairs to be large enough to accommodate the bound ligand and elongate the double helix, resulting in an increase of BSA viscosity while a non-classical intercalation or a groove mode would reduce the

Table 2. The thermodynamic parameters for the NTF binding to BSA at different temperatures

T (K)	ΔG^0 (kJ mol ⁻¹)	ΔH^0 (kJ mol ⁻¹)	ΔS^0 (J mol ⁻¹ K ⁻¹)
293	-20.36		125.31
303	-21.51	16.35	124.98
310	-22.56		126.00

BSA viscosity [32]. The viscosity measurements were taken by varying the concentration ratio of BSA and NTF. The values of relative specific viscosity $(\eta/\eta_0)^{1/3}$ vs. [NTF]/[BSA] were plotted in the absence and presence of BSA as shown in figure 6.

**Figure 6.** Effect increasing the concentration of BSA on the relative viscosity of NTF.

As it was observed from figure, the relative specific viscosities of BSA exhibited a dependence on the concentration of NTF, which increases with the value of [NTF]/[BSA]. The behaviour indicates that non-classical intercalation mode of binding and possibly a groove binding *via* hydrophobic interaction between NTF with BSA.

Molecular Modeling study: Molecular modeling has been employed to study of the interaction between NTF and BSA. The NTF was docked to BSA to determine the favoured binding site and binding mode. The best confirmation was determined based on binding affinity and RMSD. The binding energy and RMSD was performed by Auto Dock Vina. The crystal structure of BSA (Figure 7) contains 583 amino acid residues in a single polypeptide chain. It is known to have heart shaped structure with net charge of -16 on its surface and contains three homologous domains (I, II, and III): I (residues 1-183), II (184-376), III (377-583), [33, 34] and each containing two sub domains (A and B). The two sub domains form a cylindrical structure and almost all the hydrophobic amino acids surrounded in the cylindrical chamber to form the hydrophobic cavity [35]. The most important regions of ligand binding to BSA are located in hydrophobic cavity in sub domains IIA and IIIA, which is consistent with sites I and II respectively.

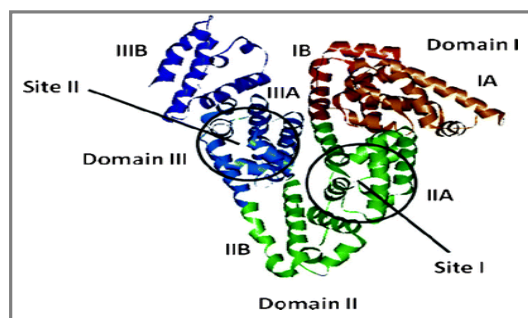
**Figure 7.** The crystallographic structure of BSA.

Figure 8 and 9 displayed the molecular docking of NTF and only amino acids residues surrounded NTF were shown. It can be seen from figure 8 and 9, NTF molecules in the subdomain IIA and IIIA cavity of BSA, in which there was a large hydrophobic region which can hold many drugs. The number of dotted lines linking amino acids represented hydrogen bonds. The presence of hydrogen bonds possibly enhanced the hydrophobicity of NTF-BSA system, making NTF-BSA system be a stable state. The whole molecule of NTF embedded into a hydrophobic cavity formed by TRP-212 residue, LEU-196, LEU-345, LEU-451 residues, Arginine (ARG-193, ARG-197, ARG-482, ARG-483) residues, Tyrosine (THR-450) and other amino acid residues. There are two hydrogen bonds between the NTF (oxygen groups) and the amino acid residues of BSA; they are -C = O and TYR-147 with a bond length of 3.0°A, -C = O group and SER-192 with a bond length of 3.0°A. Thus, the binding forces to keep NTF-BSA system stable was conjectured predominantly hydrophobic interaction as well as hydrogen bonds. The energy obtained $-9.4 \text{ k cal mol}^{-1}$ for NTF-BSA complex.

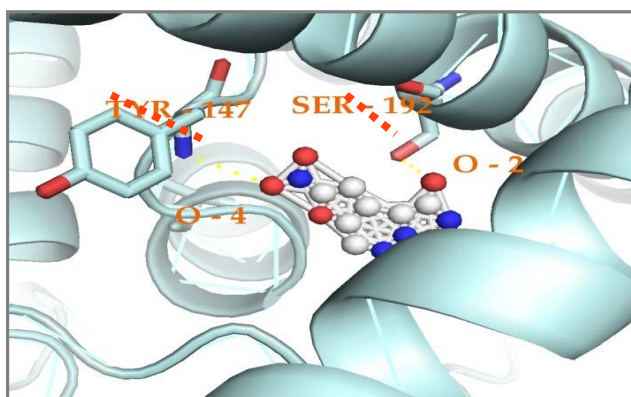


Figure 8. The hydrogen bond interaction (Red dashed line) between NTF (stick) and BSA (cartoon).

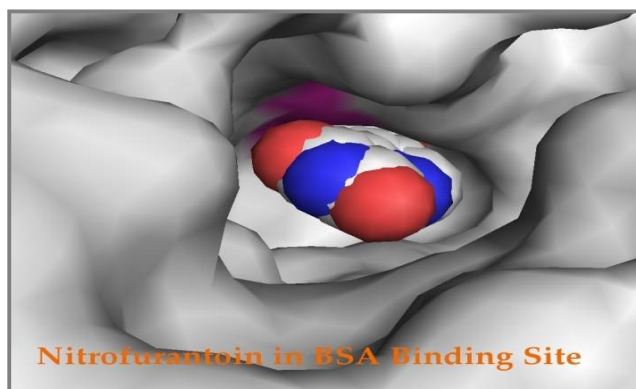


Figure 9. Molecular docked model of NTF (sphere representation) located within the hydrophobic pocket of BSA.

APPLICATION

The present work provides various methodologies to understand the mechanism of interaction of pharmaceutically important drug, NTF with biomolecule, BSA.

CONCLUSION

In the present research work, the interaction of NTF with BSA was studied by UV-Vis in combination with fluorescence spectroscopy, Viscometric and molecular modeling techniques under the

physiological condition. We have investigated that fluorescence quenching mechanism of NTF by BSA is a static quenching mechanism; $K_{sv} = 3.338 \times 10^3 \text{ L mol}^{-1}$, $k_q = 3.3375 \times 10^{11} \text{ L mol}^{-1}\text{s}^{-1}$ and $K_b = 4.275 \times 10^3 \text{ L mol}^{-1}$. The results of thermodynamic parameters obtained indicated that hydrophobic force and hydrogen bond were predominant forces to be stable the NTF-BSA complex. According to the results obtained from UV-Vis absorption spectrum suggested that the conformation of BSA changed when combining with NTF. Furthermore, molecular modeling studies revealed that the NTF was in the sub-domain IIA and IIIA of the BSA. This work should be helpful for the understanding the interaction of NTF with DNA and designing new drugs.

ACKNOWLEDGEMENT

The authors are grateful for Maharani's Science College for Women, Palace Road, Bangalore for having DST- FIST, STAR-DBT, UGC-CPE Facilities.

Conflict of interest: The authors declare that they have no conflict of interest.

REFERENCES

- [1]. E. La'zaro, P. J. Lowe, X. Briand, B. Faller, New approach to measure protein binding based on a parallel artificial membrane assay and human serum albumin, *J Med Chem*, **2008**, 51, 2009-2017.
- [2]. F. Bosca, Seeking to shed some light on the binding of fluoroquinolones to albumins, *J Phys Chem B*, **2012**, 116,3504-3511
- [3]. P. Bolel, S. Datta, N. Mahapatra, Halder M Spectroscopic investigation of the effect of salt on binding of tartrazine with two homologous serum albumins: quantification by use of the Debye-Hu'ckel limiting law and observation of enthalpy-entropy compensation, *J Phys Chem B*, **2012**, 116,10195-10204.
- [4]. X. M. He, D. C. Carter Atomic structure and chemistry of human serum albumin, *Nature*, **1992**, 358, 209-215.
- [5]. N. Gull, P. Sen, R. H. Khan, Kabir-ud-Din Interaction of bovine (BSA), rabbit (RSA), and porcine (PSA) serum albumins with cationic single-chain/gemini surfactants: a comparative study. *Langmuir*, **2009**, 25, 11686-11691
- [6]. N. Gull, S. Kumar, B. Ahmad, R. H. Khan, Kabir-ud-Din Influence of urea additives on micellar morphology/protein conformation, *Colloid Surf B*, **2006**, 51, 10-15
- [7]. P. Sen, B. Ahmad, R. H. Khan, Formation of a molten globule like state in bovine serum albumin at alkaline pH, *Eur Biophys J*, **2008**, 37, 1303-1308.
- [8]. Mallappa M, Savanur AM, Gowda BG, Vishwanth RS and Bijesh P, Molecular Interaction of Hemorrhheologic Agent, Pentoxifylline with Bovine Serum Albumin: An Approach to Investigate the Drug Protein Interaction Using multispectroscopic, voltammetry and Molecular Modelling Techniques. *Z. Phy. Chem.*, **2018** (2), 1-22.
- [9]. E. Ahmad, P. Sen, R. H. Khan Structural stability as a probe for molecular evolution of homologous albumins studied by spectroscopy and bioinformatics, *Cell Biochem Biophys*, **2011**, 61, 313-325.
- [10]. G. K. Wang, X. Li, X. L. Ding, D. C. Wang, C. L. Yan, Y. Lu, Exploring the mechanism of interaction between 5-(ethoxycarbonyl)-6-methyl-4-(4-methoxyphenyl)-3,4-dihydropyrimidin-2(1H)-one and human serum albumin: spectroscopic, calorimetric and molecular modeling studies, *J Pharm Biomed Anal.*, **2011**, 55,1223-1226.
- [11]. Mallappa M, Gowda BG, Jayanth IG, Raghavendran R, Spectroscopic, voltammetry and molecular docking study of binding interaction of antipsychotic drug with bovine serum albumin, *J. Electrochem. Sci. Eng.* **2016**, 6(2) 155-164.
- [12]. Y. Zhang, J. H. Li, X. R. Liu, F. L. Jiang, Y. Liu, Biophysical studies on the interactions of a classic mitochondrial uncoupler with bovine serum albumin by spectroscopic, isothermal titration calorimetric and molecular modeling methods, *J Fluoresc.*, **2011**, 21, 475-485.

- [13]. Gowda BG, Mallappa M., Hadimani CC, Spectroscopic and viscositic studies on the interaction of solifenacin succinate with DNA, *Asian J. Biomed. and Pharm. Sci.*, 04(35), **2014**, 44-48.
- [14]. G. K. Mcevor, AHFS Drug Information, *American Society of Hospital Pharmacists.*, **1990**.
- [15]. G. M. Morris, D. S. Goodsell, R. S. Halliday, Automated docking using a Lamarckian genetic algorithm and an empirical binding free energy function, *J Compu Chem.*, **1998**, 19 (14),1639-1662.
- [16]. T. R Alasdair, Laurie, Richard M. Jackson, Q-Site Finder: an energy-based method for the prediction of protein–ligand binding sites, *Bioinformatics*, **2005**, 21(9), 1908-16.
- [17]. Noel M O’Boyle, Michael Banck, Open Babel: An open chemical toolbox, *Journal of Cheminformatics.*, **2011**, 3, 33.
- [18]. O. Trott, A. J. Olson, AutoDock Vina: improving the speed and accuracy of docking with a new scoring function, efficient optimization and multi threading, *J. Compu. Chem.*, **2010**, 31, 455-461.
- [19]. R. Fukuda, S. Takenaka, M. Takagi, Metal ion assisted DNA-intercalation of crown ether-linked acridine derivatives, *J. Chem. Soc. Chem. Commun.*, **1990**, 1028-1030.
- [20]. P. Yang, C. Q. Zhou, Study on the interaction between calcein and herring sperm BSA by spectrophotometry, *Acta chimica sinica.*, **2003**, 61,1455-1460.
- [21]. X. L. Wang, H. Chao, H. Li, X. L. Hong, Y. J. Liu, L. F. Tan, L. N. Ji , *J. Inorg. Biochem.*, **2004**, 98, 1143.
- [22]. S. Ashoka, J. Seetharamappa, P. B. Kandagal, S. M. T. Shaik, Investigation of the interaction between trazodone hydrochloride and bovine serum albumin, *J Lumin.*, **2006**, 121, 179-186.
- [23]. J. R. Lakowicz, G. Weber, Principles of fluorescence spectroscopy, *Plenum.*, New York, **1999**.
- [24]. J. R. Lakowicz, G. Weber, Quenching of fluorescence by oxygen Probe for structural fluctuations in macromolecules, *Biochemistry*, **1973**, 12, 4161-4170.
- [25]. W. R. Ware, Oxygen quenching of fluorescence in solution an experimental study of the diffusion process, *J. Phys. Chem.*, **1962**, 66, 455-458.
- [26]. Y. Y. Yue, Y. H. Zhang, L. Zhou, J. Qin, X. G. Chen, In vitro study on the binding of herbicide glyphosate to human serum albumin by optical spectroscopy and molecular modeling, *J Photochem Photobiol B*, **2008**, 90, 26-32.
- [27]. F. L. Cui, L. X. Qin, G. S. Zhang, X. J. Yao, J. Du, Binding of daunorubicin to human serum albumin using molecular modeling and its application, *Int. J. Macromol*, **2008**, 42, 221-228.
- [28]. S. Y. Bi, D. Q. Song, Tian Y, X. Zhou, Z. Y. Liu, H. Q. Zhang, Molecular spectroscopic study on the interaction of tetracyclines with serum albumins, *Spectrochim Acta Part A.*, **2005**, 61, 629-636.
- [29]. N. Juziro, M. Noriko, Binding parameters of theophylline and aminophylline to bovine serum albumin. *Chem Pharm Bull.*, **1985**, 33, 2522-2524.
- [30]. Maidul Islam Md, Maharudra Chakraborty, Prateek, Abdulla Al Masum, Neelima Gupta, Subrata Mukhopadhyay Binding of DNA with Rhodamine B: Spectroscopic and molecular modeling studies, *Dyes and Pigments.*, **2013**, 99, 412-422.
- [31]. Jin Lian Zhu, Jia He, Hua He, Shu Hu Tan, Xiao Mei He, Chuong Pham-Huy, Lun Li., Study on the interaction between ketoprofen and bovine serum albumin by molecular simulation and spectroscopic methods, *Spectroscopy*, **2011**, 26, 337-348.
- [32]. Hao-Yu Shen, Xiao-Li Shao, Hua Xu, Jia LI, Sheng-Dong. Pan In Vitro Study of BSA Interaction with Trichlorobenzenes by Spectroscopic and Voltammetric Techniques, *Int. J. Electrochem. Sci.*, **2011**, 6, 532-547.
- [33]. J. Jayabharathi, K. Jayamoorthy, V. Thanikachalam, Docking investigation and binding interaction of benzimidazole derivative with bovine serum albumin, *J. Photochem. and Photobiol. B: Biology*, **2012**, 117, 27-32.
- [34]. Satyajit Patra, Kotni Santhosh, Ashok Pabbathi, Anunay Samanta, Diffusion of organic dyes in bovine serum albumin solution studied by fluorescence correlation spectroscopy, *RSC Adv.*, **2012**, 2, 6079-6086.
- [35]. Z. Q. Jiang, Y. H. Chi, J. Zhuang, *Spectrosc.spect.Anal.*, **2007**, 27, 986-990.